Resonance Raman Spectroelectrochemistry. 3. Tunable Dye Laser Excitation Spectroscopy of the Lowest $^2B_{1u}$ Excited State of the Tetracyanoquinodimethane Anion Radical

David L. Jeanmaire and Richard P. Van Duyne*[1]

Contribution from the Department of Chemistry, Northwestern University, Evanston, Illinois 60201. *Received September 8, 1975*

Abstract: Resonance Raman (RR) excitation spectra have been measured for the ν_2, ν_4, ν_5, and ν_9 totally symmetric normal modes of the tetracyanoquinodimethane monoanion radical using the hybrid technique of resonance Raman spectroelectrochemistry (RRSE). A CW tunable dye laser was used as the excitation source in these experiments to cover an excitation region of 15 000 to 17 850 cm^{-1} within the $^2B_{3g} \rightarrow {}^2B_{1u}{}^{(1)}$ transition of $TCNQ\cdot^-$. These spectra reveal a substantial amount of vibronic fine structure information. An analysis of the excitation spectra has been carried out leading to frequency assignments for the electronic structure sensitive ν_2' (C≡N stretch) and ν_4' (C=C ring stretch + C=C wing stretch) modes in the $^2B_{1u}{}^{(1)}$ excited state.

Resonance Raman (RR) spectroscopy is strikingly distinguished from normal Raman (NR) spectroscopy by the great sensitivity of its observables to changes in the laser excitation wavelength. In particular this is manifested by the following: (1) a subset of the normal Raman active vibrational modes exhibits intensity enhancement factors of up to 10^6 when the excitation wavelength falls within an electronic absorption band; (2) the intensities of these resonance Raman active modes are strong functions of the excitation frequency, ν_0, and do not follow the ν_0^4 dependence of NRS; and (3) inverse polarization (antisymmetric scattering) as well as polarization dispersion can be observed in molecules of appropriate molecular point group. By continuously scanning the laser excitation wavelength from a region of zero sample absorbance into and through an electronic absorption band it is possible (i.e., only laser technology limited) to vary an observed Raman signal from one characteristic of NR to one characteristic of RR passing through an intermediate preresonance (PR) state. Considerable effort, both theoretical and experimental, has already been expended in order to develop a detailed picture of the dependence of Raman scattering intensity on the excitation frequency. The vibronic theory of Raman scattering, based on the application of the Kramers–Heisenberg–Dirac (KHD) dispersion equation to molecular systems,[2] has been developed by Albrecht,[3] Savin,[4] Verlan,[5] and others[6-9] to describe the wavelength dependence of Raman intensity in the PR region. Common to these treatments is the incorporation of the adiabatic Born–Oppenheimer approximation and the Herzberg–Teller description of vibronic activity into the KHD dispersion equation. Experimental validation of these treatments for the PR region has been reasonably successful.[10,11] Recently Siebrand and Mingardi[12,13] have pointed out that these "standard" Raman intensity vs. excitation wavelength treatments break down near and in resonance due to convergence problems in the schemes used to effect the sum over the vibrational levels of the resonant excited state. These authors have advanced a more detailed treatment of this problem in which the convergence difficulties in the excited state vibrational sum are avoided and nonadiabatic coupling terms are retained for generality. A related approach has been formulated independently by Van Labeke, Jacon, Berjot, and Bernard.[14]

Experimental evidence for the validity of these formulations of the theory of resonance Raman scattering can be obtained most directly from the study of resonance Raman excitation spectra, i.e., the intensity of a particular Raman line plotted as a function of laser excitation frequency. Mingardi, Siebrand, Van Labeke, and Jacon[15] have used the theory to calculate excitation spectra for totally symmetric modes, compare them with the corresponding electronic absorption spectrum, and compare these theoretical predictions with the available experimental data for MnO_4^-. In general the theory suggests the following rule: *The excitation spectrum of a particular normal mode should roughly parallel the absorption spectrum.* This rule is in agreement with the observation that RR scattering occurs only when there is absorption of the excitation light and the scattering is stronger the stronger the absorption. For totally symmetric modes this rule will be most closely followed in cases where: (1) the molecule has only one totally symmetric mode or (2) the electronic absorption spectrum shows essentially no vibronic fine structure due to the merging of strongly overlapping excited state vibrational levels. On the other hand for molecules having several totally symmetric modes and either partially or fully resolved vibronic structure in the absorption spectrum, the possibility exists that RR excitation spectra will show a series of resonances having similar vibrational spacing as the absorption spectrum but quite a different intensity distribution. Thus in certain cases one may be able effectively to resolve the absorption spectrum by monitoring the intensity of Raman lines corresponding to different totally symmetric normal modes as a function of ν_0. At the present time experimental data which unambiguously demonstrate this feature of RR exciation spectra are quite limited. This is largely due to the coarse wavelength spacing of data points imposed by the use of multiple line, fixed frequency lasers such as Ar^+ or Kr^+ for excitation profile studies.

In this work we wish to report a preliminary study of resonance Raman excitation spectra for certain of the totally symmetric normal modes of the electrogenerated tetracyanoquinodimethane radical anion ($TCNQ\cdot^-$). The RR scattering spectrum, electronic absorption spectrum, and electrochemical properties of $TCNQ\cdot^-$ are discussed in the preceding paper.[16] The RR excitation spectra are all obtained by excitation into the region of the lowest doublet excited state ($^2B_{1u}{}^{(1)}$) of $TCNQ\cdot^-$ (D_{2h}, Y axis parallel to the long C_2 axis, Z axis perpendicular to the molecular plane) with an Ar^+ pumped CW "jet-stream" dye laser. This laser can be tuned continuously over a 2850-cm^{-1} region within the $^2B_{3g} \rightarrow {}^2B_{1u}{}^{(1)}$ transition (15 000 to 17 850 cm^{-1}).

Experimental Section

Purification of materials, sample preparation, electrochemical

methodology, and the apparatus for carrying out resonance Raman spectroelectrochemistry (RRSE) experiments in the controlled potential electrolysis electrogeneration mode for the purpose of obtaining RR scattering spectra have been previously described.[16,17]

Resonance Raman excitation spectra are plots of the intensity of a particular RR line in the scattering spectrum relative to the intensity of an NR internal standard line (typically a solvent line) as a function of the laser excitation frequency, ν_0. This relative intensity, $I_{rel}(\nu_0)$, is independent of experiment to experiment variations in laser power and sample concentration. However, $I_{rel}(\nu_0)$ must be corrected for the effects of self-absorption and spectrometer sensitivity, which are both functions of ν_0, before it can be meaningfully related to its theoretically calculable counterpart, the molar scattering cross section, $\alpha(\nu_0)$. The corrected relative intensity is given by:[18,19]

$$I_{\text{rel corr}}(\nu_0) = \frac{I(\nu_{RS})C_S{}^0\nu_S{}^4}{I^0(\nu_S)C_{RS}\nu_{RS}{}^4}\left[\frac{S^0(\nu_S)}{S(\nu_{RS})}\right]\left\{\frac{[\epsilon(\nu_0)+\epsilon(\nu_{RS})]}{[\epsilon(\nu_0)+\epsilon(\nu_S)}\right.$$
$$\left.\times\frac{[1-10^{-bC_{RS}[\epsilon(\nu_0)+\epsilon(\nu_S)]}]}{[1-10^{-bC_{RS}[\epsilon(\nu_0)+\epsilon(\nu_{RS})]}]}\right\} = \frac{\alpha(\nu_0)}{\alpha^0} \quad (1)$$

where $I(\nu_{RS})$ is the experimentally measured intensity (i.e., fully resolved, background corrected peak height) for the resonance enhanced line whose scattered frequency is ν_{RS} ($\nu_{RS} = \nu_0 - \Delta\nu_{RS}$); C_{RS} is the molar concentration of the resonant scatterer; and $S(\nu_{RS})$ is the spectrometer sensitivity factor at ν_{RS}. $I^0(\nu_S)$, C^0, and $S^0(\nu_S)$ are the corresponding quantities for the nonresonance enhanced line of the internal standard whose scattered frequency is ν_S ($\nu_S = \nu_0 - \Delta\nu_S$). The expression in braces is the self-absorption correction derived by Shriver and Dunn[19] for the backscattering geometry used in these experiments. α^0 is the ν_0 independent molar scattering cross section for the NR internal standard line. $\epsilon(\nu_0)$, $\epsilon(\nu_S)$, and $\epsilon(\nu_{RS})$ are the extinction coefficients of the resonant scatterer at ν_0, ν_S, and ν_{RS}.

RR excitation spectra were acquired using a Spex Model 1400-II double monochromator equipped with a cooled RCA C31034 photomultiplier tube and standard low-level threshold photon counting detection electronics. The excitation source was a Coherent Radiation Laboratories (CRL) Model 490 CW tunable dye laser pumped by the CRL Model CR-8 Ar^+ laser. The dye laser was manually scanned in 2.0, 5.0, or 20.0-Å increments over the range 5600 to 6667 Å depending on the excitation resolution desired. This range of excitation wavelengths was achieved using sodium fluorescein (NaFl), rhodamine 6G (R6G), and rhodamine B (RB) dye solutions. 1,3,5,7-Cyclooctatetraene (COT) purchased from Aldrich Chemical Co. and used without purification was added to the NaFl and RB dye solutions. COT acts as a quenching agent for the laser dye triplet state[20] and thereby lowers the pumping threshold, extends the tuning range of the dye, and improves overall pump to dye laser conversion efficiency. NaFl would not lase at all (up to 8 W all lines pump power) without the addition of COT. In the case of RB, which lases moderately well without COT (ca. 500 mW at 6200 Å pumped by 8 W all lines), the tuning curve peak was shifted from 6200 Å to approximately 6350 Å and the output power at 6350 Å increased to ca. 1.3 W with 8 W all lines pumping on the addition of 3 ml of neat COT to the 1.5 l. dye solution. A premonochromator was used to remove the superradiant fluorescence emission from the dye laser output beam as described previously.[16] The procedure for collecting the RR excitation data involves: (1) electrogenerating a 1.0-3.0 × 10^{-3} M solution of $TCNQ\cdot^-$ in acetonitrile containing 0.10 M tetrabutylammonium perchlorate; (2) setting the dye laser to the desired ν_0 and optimizing the output power; (3) adjusting the premonochromator for maximum dye laser throughput; and (4) scanning the double monochromator over a 150- to 500-cm^{-1} range to record a partial Raman scattering spectrum which includes the background in that range, the $TCNQ\cdot^-$ RR line of interest, and the CH_3CN NR line nearest the $TCNQ\cdot^-$ line. The NR lines serve as the internal standards for the $TCNQ\cdot^-$ intensity measurements. Since $TCNQ\cdot^-$ solutions are not infinitely stable (i.e., they decay by about 5% over a period of 5-7 h) intensity measurements were made at only 20-25 different values of ν_0 per electrogeneration.

For purposes of direct comparison with the RR excitation spectra, a portion of the $TCNQ\cdot^-$ electronic absorption spectrum from ca. 500 to 660 nm was scanned on a Cary Model 14 Spectrophotometer fitted with a Dumont Model 7664 photomultiplier tube and a retransmitting slidewire. The voltage output from the slidewire, which is proportional to absorbance, was voltage-to-frequency converted, counted for 1.00-s intervals, and recorded on magnetic tape of a BCD number. This digitized absorption spectrum was then replotted in linear wavenumber format chosen to match that for the excitation spectra.

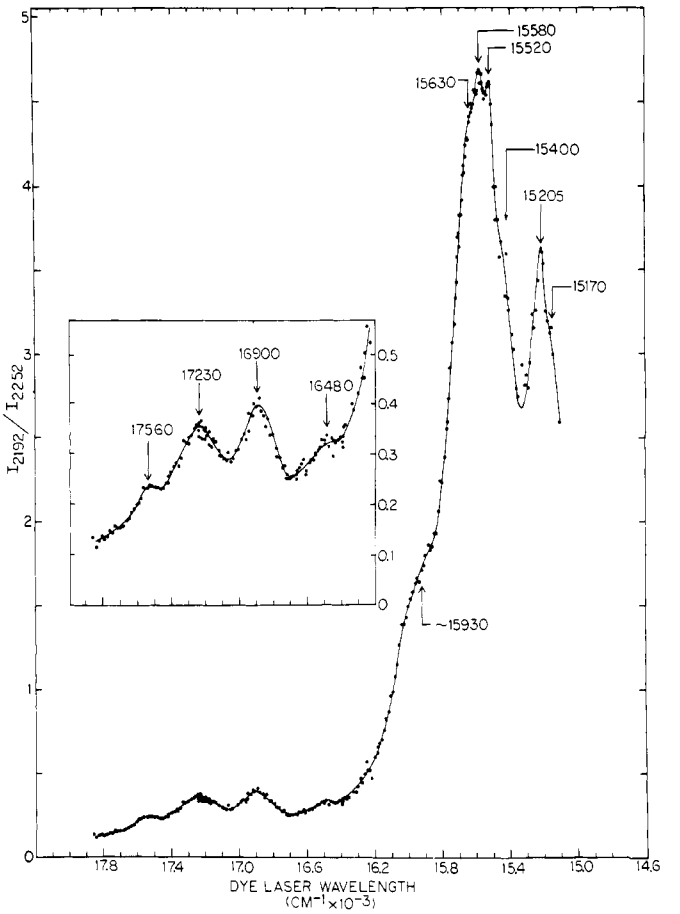

Figure 1. Resonance Raman excitation spectrum of the ν_2 (C≡N stretch) mode of electrogenerated $TCNQ\cdot^-$ at 2192 cm^{-1}. The inset shows the 16 200 $cm^{-1} \leq \nu_0 \leq$ 17 850 cm^{-1} excitation region with a 3× expanded relative intensity scale. 1.0 mM ≤ [$TCNQ\cdot^-$] ≤ 3.0 mM.

Results and Discussion

$^2B_{3g} \rightarrow {}^2B_{1u}(1)$ RR Excitation Spectra for the ν_2, ν_4, ν_5, and ν_9 Modes of $TCNQ\cdot^-$. Resonance Raman excitation spectra for the ν_2 totally symmetric C≡N stretching mode at $\Delta\nu_{RS}$ = 2192 cm^{-1} and the ν_3 totally symmetric bending mode (C–C–C ring bend + C—C≡N bend) at $\Delta\nu_{RS}$ = 336 cm^{-1} of electrogenerated $TCNQ\cdot^-$ are presented in Figures 1 and 2. The depolarization ratios for ν_2 and ν_9 were 0.32 ± 0.02 and were independent of the exciting wavelength. These two $TCNQ\cdot^-$ fundamentals were chosen for this preliminary investigation of RR excitation spectroscopy due to their proximity to the NR CH_3CN lines at $\Delta\nu_S$ = 2252 cm^{-1} and $\Delta\nu_S$ = 379 cm^{-1}. Since $\nu_{RS} \cong \nu_S$ for these two pairs of lines, and both the spectrometer and detector sensitivity factors as well as the $TCNQ\cdot^-$ extinction coefficient are not extremely sensitive functions of ν_0 in the 550–660-nm region, eq 1 is well approximated by:

$$\alpha(\nu_0) = \left[\frac{\alpha^0 C_S\nu_S{}^4}{C_{RS}\nu_{RS}{}^4}\right]\frac{I(\nu_{RS})}{I^0(\nu_S)} \quad (2)$$

Under these experimental circumstances spectrometer/detector sensitivity and self-absorption corrections do not have to be made on a point by point basis. This represents a considerable simplification in the data reduction procedure since for the excitation spectra in Figures 1 and 2 it would have been necessary to calculate over 350 self-absorption and spectrometer/detector sensitivity corrections. Clearly some form of automated data reduction will in general be necessary in

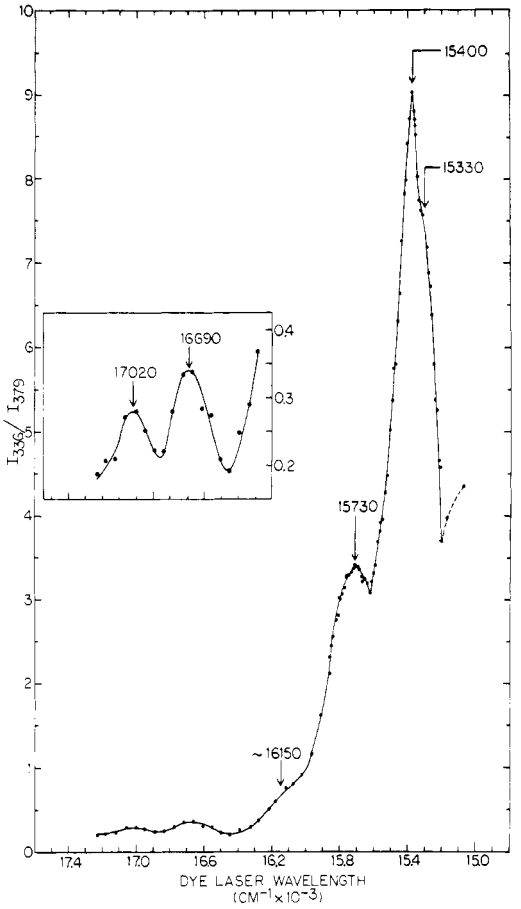

Figure 2. Resonance Raman excitation spectrum of the ν_9 (C-C-C ring bend + C—C≡N bend) mode of electrogenerated TCNQ·$^-$ at 336 cm^{-1}. The inset shows the 16 200 $cm^{-1} \leq \nu_0 \leq$ 17 400 cm^{-1} excitation region with a 5× expanded relative intensity scale. 1.0 mM ≤ [TCNQ·$^-$] ≤ 3.0 mM.

order to efficiently produce corrected excitation spectra unless there is so little structure in a given spectrum that 10–20 data points are sufficient to define the spectral profile.

Several experimental RR excitation studies have now been carried out and can be compared with the RR excitation spectra of TCNQ· $^-$reported here on the basis of: (1) resolution (i.e., number of corrected relative intensity measurements per 1000 cm^{-1} ν_0 interval); (2) number and spacing of intensity maxima; (3) resonance line width; (4) similarity of the excitation spectra for different normal modes; and (5) relationship between the electronic absorption spectrum and the RR excitation spectra. Excluding excitation experiments confined to the preresonance region, these studies have concentrated on small inorganic and large biomolecular systems. The inorganic systems studied extensively possess only one totally symmetric RR active mode, e.g., MnO_4^-,[21] MoS_4^{2-},[22] and I_2.[24,25] In contrast the biomolecule systems and related model compounds have a very large number of both totally symmetric and nontotally symmetric RR active modes, e.g., the heme proteins,[25] carotenoids,[26,27] cobalamins,[28] and iron(III) transferrin.[29] The TCNQ radical anion represents an intermediately sized molecule with ten totally symmetric RR active modes (only seven of which are actually observed in the $^2B_{1u}{}^{(1)}$ scattering spectrum).[16] The present study of RR excitation spectroscopy was initiated partly on the suspicion that certain general features of the resonance Raman phenomenon might be more readily observed in a molecule of intermediate complexity than in either the small or large molecule limit.

With regard to excitation resolution, the TCNQ·$^-$ spectra in Figures 1 and 2 have been acquired at a factor of 20–30 higher resolution than any previously reported. The 2192-cm^{-1} excitation spectrum consists of ca. 90 intensity measurements per 1000 cm^{-1} and 336-cm^{-1} spectrum consists of ca. 45 per 1000 cm^{-1}. These values can be compared with the resolution of the 1600-cm^{-1} band of Fe(EDDHA)$^-$ [29] which is ca. 3 intensity measurements per 1000 cm^{-1} and is characteristic of the highest resolution excitation spectrum previously reported.

As a consequence of carrying out the TCNQ·$^-$ excitation experiments at "high" resolution, we were able to locate seven intensity maxima and four shoulders in the ν_2 spectrum as well as four maxima and two shoulders in the ν_9 spectrum. Thus more extensive vibronic fine structure has now been observed in these two TCNQ·$^-$ excitation spectra than in the iron(III) transferrin or Fe(EDDHA)$^-$ systems which until now had exhibited the greatest vibronic structure content. Another unique feature of the spectra in Figures 1 and 2 is that the intensity maxima do not form a uniformly spaced progression as was the case in the iron(III) transferrin system. Clearly more than one excited state vibrational mode is involved in forming this resonance Raman scattering pattern. This is likely to be a direct consequence of the fact that we are pumping TCNQ·$^-$ in the high-energy "tail" of the $^2B_{3g} \rightarrow {}^2B_{1u}{}^{(1)}$ transition where it is more likely to excite levels containing quanta of more than one vibrational mode than if excitation were confined to the zero point level region.

One further observation resulting from these "high" resolution excitation studies on TCNQ·$^-$ is that the line width of a resonance in RR spectroscopy can be reasonably narrow. As can be seen in the ν_2 excitation spectrum (Figure 1), it is possible to partially resolve intensity maxima whose peak frequencies differ by only 60 cm^{-1}. This indicates that resonance line widths in TCNQ·$^-$ may be on the order of only 100–200 cm^{-1} in this medium. In other systems resonance line widths on the order of 750–1000 cm^{-1} have been observed;[28] however, in some instances this large a line width may be a consequence of the "low" resolution of the excitation measurements. It is probably not possible to significantly improve the resolution observed between the 15 580- and 15 520-cm^{-1} peaks in the ν_2 spectrum by making more intensity measurements with finer ν_0 spacing since the laser line width is ca. 1.0 cm^{-1} in this spectral region. Also it should be pointed out that the resolution achieved in Figure 1 between the 15 580- and 15 520-cm^{-1} maxima was made possible by counting for four times longer on the intensity measurements in this region in order to effect an increase in the signal-to-noise ratio. Additional resolution improvement may be possible using a combination of an intracavity etalon to narrow the laser line (at the expense of a reduction in output power) and low sample temperature to remove the influence of ν_9 hot bands.

Next we compare the mode to mode similarity of the TCNQ·$^-$ excitation spectra with that of other systems having more than one RR active mode. Theoretically one expects that different subsets of the RR active modes in the scattering spectrum will contribute to form the resonance Raman scattering pattern manifested in the excitation spectra.[13,15] Therefore it should be possible in certain cases to further resolve an electronic absorption spectrum by monitoring the RR excitation spectra of all active modes. This expectation is nicely illustrated by the apparent complementarity of the ν_2 and ν_9 excitation spectra in Figures 1 and 2. Everywhere there is an intensity maximum in the ν_2 spectrum there is a minimum or weak shoulder in the ν_9 spectrum. This complementarity feature of the excitation spectra is emphasized in Figure 3B which shows their superposition. The $I_{rel}(\nu_0)$ axis has been arbitrarily scaled to 0.0–10.0 for all the excitation spectra in Figure 3B in order to facilitate comparison of their relative shapes. We also want to point out that this feature of excitation spectrum complementarity could account for the intensity behavior of the 540-cm^{-1} RR band in the TCNE·$^-$ system when the ex-

citation wavelength was changed from 4765 to 4579 Å.[17] By comparison with the excitation spectra for $TCNQ\cdot^-$, the mode to mode excitation spectrum differences are much less striking in other systems. For example, in the heme proteins and β-carotene, one observes the same number of intensity maxima in all excitation spectra and in general the peak positions are only slightly displaced from one spectrum to another. An exception to this occurs in the case of ferrihemoglobin fluoride[25] in which the 1373-cm^{-1} excitation profile shows no peak when laser excitation is in the region of the Q_{0-0} and Q_{0-1} bands but shows a monotonic intensity increase; whereas, the 1340-, 1175-, and 760-cm^{-1} excitation spectra exhibit intensity maxima corresponding to the Q_{0-1} electronic band. The 1373-cm^{-1} RR line is presumably in preresonance with the Soret band. The iron(III) transferrin and $Fe(EDDHA)^-$ systems studied by Spiro et al., on the other hand, do show some hints of complementary excitation spectra (viz., the $Fe(EDDHA)^-$ 637-cm^{-1} excitation spectrum shows a maximum at ν_0 = 20 400 cm^{-1} and the other spectra show lower intensity shoulders at this position).

Figure 3 also details the relationship between the electronic absorption spectrum of $TCNQ\cdot^-$ and the excitation spectra for ν_2 and ν_9 in the range 15 000–17 850 cm^{-1}. In addition we show "low" resolution excitation spectra for two other modes: ν_4 (C=C ring stretch + C=C wing stretch) at $\Delta\nu_{RS}$ = 1389 cm^{-1} and ν_5 (C–H bend) at $\Delta\nu_{RS}$ = 1195 cm^{-1}. Self-absorption and spectrometer sensitivity corrections have not been made for the ν_4 and ν_5 excitation spectra. However, calculations made comparing eq 1 and 2 in the region of the ν_4 and ν_5 excitation spectra intensity maxima show that an error of less than 10 cm^{-1} peak location is made by ignoring these corrections. The relative intensities of the various bands in the ν_4 and ν_5 excitation spectra are, however, substantially altered by self-absorption correction. From Figure 3 it is evident that significantly more vibronic structure information is resolved in the collection of RR excitation spectra than the corresponding electronic absorption spectrum for the $TCNQ\cdot^-$ system. This demonstrates that RR excitation spectroscopy may have the potential to develop into a powerful tool for the study of vibronic spectroscopy. It should also be pointed out that in the iron(III) transferrin and $Fe(EDDHA)^-$ systems more vibronic structure was found in the excitation spectra than in the electronic absorption spectrum. In other systems such as some of the heme proteins and β-carotene the vibronic information content was only slightly greater than that contained in the absorption spectrum.

Assignment of the RR Excitation Spectra. Assignment of the intensity maxima in the $TCNQ\cdot^-$ excitation spectra of ν_2, ν_4, ν_5, and ν_9 to individual vibronic levels in the $^2B_{1u}{}^{(1)}$ excited state is complicated by two experimental limitations. First, difficulty arises because complete vibronic progressions starting from the zero point level are not observable due to the restricted tuning range of our present CW dye laser in the near-infrared region. However, even if a high average power tunable CW laser existed for use in exciting the 750–900-nm region of $TCNQ\cdot^-$, a second problem would be encountered. The RCA C31034 photomultiplier tube sensitivity decreases rapidly beyond 900 nm[30] so that Raman shifted light from the higher frequency modes of $TCNQ\cdot^-$ (ν_2, ν_4, and to some extent ν_5) would be detected at greatly reduced sensitivity for λ_0 >800 nm effectively limiting the collection of RR excitation spectra on this system to the ν_9 mode. Assignment of the excitation spectra is further complicated by lack of information concerning the exact location of the zero point level and the values of the vibrational frequencies for the totally symmetric modes of $^2B_{1u}{}^{(1)}$ $TCNQ\cdot^-$.

In view of these difficulties the assignment of the ν_2, ν_4, ν_5, and ν_9 RR excitation spectra advanced in Table I should be considered tentative. For the assignment we used the notation

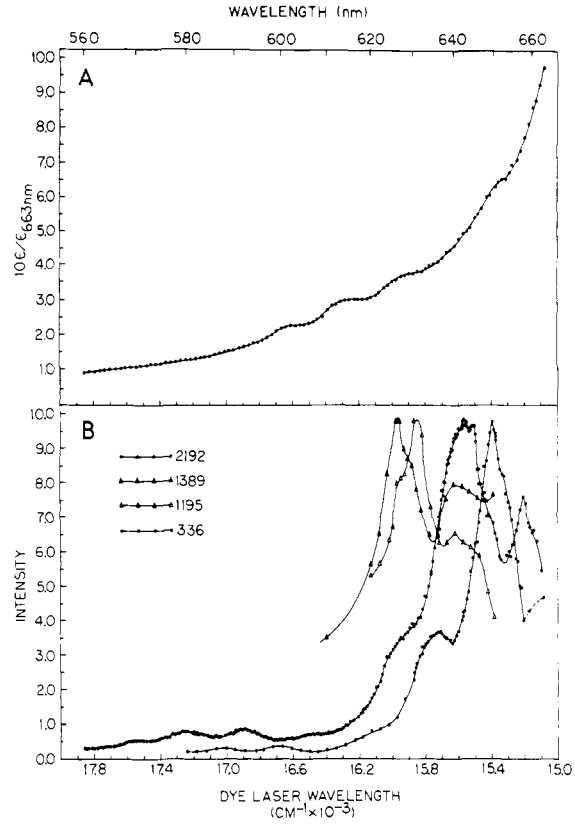

Figure 3. Comparison of $TCNQ\cdot^-$ electronic absorption spectrum and resonance Raman excitation spectra. (A) Electronic absorption spectrum from 15 000 to 17 850 cm^{-1}. The extinction coefficient, ε, scale is normalized with respect to ε at 663.0 nm (15 083 cm^{-1}) = 3.0 × 10^3 M^{-1} cm^{-1}. (B) Superposition of the ν_2 (2192 cm^{-1}), ν_4 (1389 cm^{-1}), ν_5 (1195 cm^{-1}), and ν_9 (336 cm^{-1}) excitation spectra. The relative intensity scale has been scaled to 0.0 to 10.0 for all four spectra.

introduced by Callomon, Dunn, and Mills,[31] where the number designates the vibrational mode, the subscript the number of quanta in the ground state, and the superscript the number of quanta in the excited state. The agreement between calculated and observed band maxima using this assignment is within 20 cm^{-1} for all 18 different peaks and shoulders. This is acceptable since the band maxima can be experimentally located to ∓10 cm^{-1} and the laser line width is 0.8–1.2 cm^{-1} in the 560–660-nm region. The assignment in Table I has been made on the following basis:

(1) Only those totally symmetric modes observed in the $^2B_{1u}{}^{(1)}$ scattering spectrum of $TCNQ\cdot^-$ (viz., ν_2, ν_3, ν_5, ν_7, ν_8, and ν_9) contribute to the excitation spectra.

(2) Those modes which are most strongly resonance enhanced in the scattering spectrum will make the dominant contributions to the excitation spectra. Thus the RR excitation spectra of $TCNQ\cdot^-$ have been assigned using only ν_2, ν_3, ν_4, ν_5, and ν_9.

(3) The zero point level of the $^2B_{1u}{}^{(1)}$ state can be located from the position of the first intensity maximum in the electronic absorption spectrum of $TCNQ\cdot^-$. This maximum is located by our measurements at 842 ∓ 2 nm (11 905–11 848 cm^{-1}). The value of ν_{00} leading to the best agreement between observed and calculated band positions in the excitation spectra is 11 850 cm^{-1}.

(4) The $^2B_{1u}{}^{(1)}$ excited state vibrational frequencies are: ν_2' = 2150 cm^{-1}, ν_3' = 1613 cm^{-1}, ν_4' = 1335 cm^{-1}, ν_5' = 1198 cm^{-1}, and ν_9' = 330 cm^{-1}. ν_9' and ν_4' were determined from experimental frequency differences between intensity maxima in the excitation spectra. ν_5' and ν_3' were chosen to be approximately equal to their frequencies in the $^2B_{3g}$ ground state as measured from the scattering spectrum. We feel that this

Table I. Bands Observed in the Resonance Raman Excitation Spectra of Modes ν_2, ν_4, ν_5, and ν_9 of TCNQ $\cdot^-$

Excitation spectrum of mode ν_i	Band max, cm^{-1} ($\mp$ 10)	Displacement,[a] cm^{-1}	Assignment	Displacement, calcd,[b] cm^{-1}	Δdisplacement (calcd − exptl), cm^{-1}
ν_2	15 170 (sh)	3320	$4_0^2 9_0^2$	3330	+10
ν_2	15 205	3355	$2_0^1 5_0^1$	3348	−7
ν_9	15 330 (sh)	3480	$4_0^1 2_0^1$	3485	+5
ν_2, ν_9	15 400	3550	$3_0^2 9_0^1$	3556	+6
ν_2	15 520	3670	$4_0^2 9_0^3$	3660	−10
		3670	$2_0^1 5_0^1 9_0^1$	3678	+8
ν_2	15 580	3730	$4_0^1 5_0^2$	3731	+1
ν_2, ν_4, ν_5	15 630 (sh)	3780	$3_0^1 2_0^1$	3763	−17
ν_9	15 730	3880	$4_0^2 5_0^1$	3868	−12
		3880	$3_0^2 9_0^2$	3886	+6
ν_4, ν_5	15 860	4010	$3_0^1 5_0^2$	4009	−1
ν_2	15 930 (sh)	4080	$4_0^1 5_0^2 9_0^1$	4061	−19
		4080	$3_0^1 2_0^1 9_0^1$	4093	+13
ν_4, ν_5	15 955	4105	$3_0^1 2_0^1 9_0^1$	4093	−12
ν_9	16 150 (sh)	4300	2_0^2	4300	0
ν_2	16 480	4630	$2_0^2 9_0^1$	4630	0
ν_9	16 690	4840	$4_0^2 2_0^1$	4820	−20
ν_2	16 900	5050	$4_0^2 5_0^2$	5066	+16
ν_9	17 020	5170	$4_0^2 2_0^1 9_0^1$	5150	−20
ν_2	17 230	5360	$4_0^2 5_0^2 9_0^1$	5396	+16
		5380	$2_0^1 3_0^2$	5376	−4
ν_2	17 560	5710	$4_0^2 5_0^2 9_0^2$	5726	+16

[a] ν_{00} = 11 850 cm^{-1}. [b] ν_2' = 2150 cm^{-1}; ν_3' = 1613 cm^{-1}; ν_4' = 1335 cm^{-1}; ν_5' = 1198 cm^{-1}; and ν_9' = 330 cm^{-1}.

Table II. π Bond Order Changes[a]

Bond[b]	ΔP_i: TCNQ·$^-$($^2B_{3g}$) + $h\nu_0$ → TCNQ·$^-$($^2B_{1u}^{(1)}$)	ΔP_i: TCNQ·$^-$($^2B_{3g}$) + e^- → $TCNQ^{2-}$(^1A_g)
1	+0.019	+0.032
2	−0.034	−0.051
3	+0.157	+0.182
4	−0.066	−0.100
5	+0.084	+0.081

[a] CNDO/S calculation with 70 singly excited configuration interactions, ref 33. [b] Following structure:

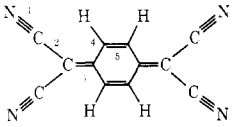

is a valid approximation since these modes are not very sensitive to changes in electronic structure as evidence by the fact that $\Delta\nu_5$ = +5 cm^{-1} and $\Delta\nu_3$ = +1 cm^{-1} for the process TCNQ·$^-$ + e^- → $TCNQ^{2-}$ ($\Delta\nu_i = \nu_i(TCNQ^{2-}) - \nu_i(TCNQ\cdot^-)$). The ground state frequencies for $TCNQ^{2-}$ were determined from the NR scattering spectrum of dilithium tetracyanoquinodimethandiide tetrahydrofuranate ($Li_2TCNQ\cdot THF$).[32] ν_2' was then determined by varying its value over the range 2102 $cm^{-1} \leq \nu_2' \leq$ 2192 cm^{-1} and selecting that value which gave the best fit between calculated and observed RR excitation band maxima. The limits of 2192 and 2102 cm^{-1} represent the ground state frequencies for ν_2 in TCNQ·$^-$ and $Li_2TCNQ\cdot$ THF, respectively.

Additional support for our excited state frequency assignments of the electronic structure sensitive modes ν_2' and ν_4' can be obtained from a comparison of the π bond order changes for TCNQ·$^-$($^2B_{3g}$) + $h\nu_0$ → TCNQ·$^-$($^2B_{1u}^{(1)}$) and TCNQ·$^-$($^2B_{3g}$) + e^- → $TCNQ^{2-}$(^1A_g). The bond order changes for these processes are listed in Table II. The bond orders were obtained from CNDO/S calculations including configuration interaction.[33]

The geometries for TCNQ and TCNQ·$^-$ were those determined by Trueblood[34] and Fritchie.[35] The $TCNQ^{2-}$ geometry was assumed to be identical with that of TCNQ·$^-$. The potential energy distribution (PED) weighted bond order changes, $\Sigma_i(PED)_{K_i}\Delta P_i$ as defined previously,[16] for ν_2 and ν_4 and +0.017 and +0.118, respectively, for the optical excitation process. The corresponding weighted bond order changes for the TCNQ·$^-$ → $TCNQ^{2-}$ transformation are +0.028 and +0.132. Since ν_2 changes from 2192 cm^{-1} in the ground state of TCNQ·$^-$ to 2102 cm^{-1} in the $TCNQ^{2-}$ ground state and the corresponding changes for ν_4 are 1389 cm^{-1} to 1300 cm^{-1}, and, in addition, the weighted bond order changes for the electron transfer are greater than for the optical excitation, it is reasonable to expect that 2102 $cm^{-1} \leq \nu_2' \leq$ 2192 cm^{-1} and 1300 $cm^{-1} \leq \nu_4' \leq$ 1389 cm^{-1}. Therefore the assigned values ν_2' = 2150 cm^{-1} and ν_4' = 1335 cm^{-1} are not unreasonable.

In the process of analyzing the RR excitation spectra, an alternative assignment, which accounted for 16 intensity maxima and shoulders within 20 cm^{-1} of the experimentally observed positions, was proposed. This assignment required ν_4' = 1240 cm^{-1} as determined from absorption maxima differences in the electronic absorption spectrum of TCNQ·$^-$. This alternative assignment was rejected on the basis of the above bond order change argument.

This preliminary study of TCNQ·$^-$ RR excitation spectroscopy will be extended to include: (1) the excitation spectra of the other modes in TCNQ·$^-$ at a resolution comparable to that presented here for ν_2 and ν_9; (2) the excitation spectra of TCNQ-d_4·$^-$ to verify assignments involving ν_5 such as 15 205 $cm^{-1} = 2_0^1 5_0^1$ in the ν_2 spectrum; and (3) the RR excitation spectroscopy of the TCNQ anion radical dimer, $(TCNQ\cdot^-)_2$, whose electronic absorption spectrum is more centered with respect to our CW dye laser tuning range than is the absorption spectrum of TCNQ·$^-$. This will permit observation of the 0–0 band region of the excitation spectrum provided that vibronic fine structure can be resolved from the structureless absorption band of $(TCNQ\cdot^-)_2$.

Conclusions

RR excitation spectra for four of the ten totally symmetric normal modes of TCNQ·$^-$ are reported here. These spectra exhibit substantial vibronic complexity. The expectation that by monitoring Raman line intensities of different modes as a function of excitation frequency an electronic absorption

spectrum can be further resolved is clearly demonstrated experimentally.

The necessity of using a continuously tunable laser with as broad a tuning range as possible for the collection of RR excitation spectra (profiles) is illustrated here. Only in situations where the vibrational levels of the resonant excited state merge into a band of strongly overlapping levels to produce very broad RR excitation spectra will it be possible to obtain other than qualitative data using the coarsely and irregularly spaced lines of a multiple line, fixed frequency laser. Use of this type of laser exclusively to study systems in which the vibronic structure is either partially or fully resolved in the electronic absorption spectrum will produce, at best, an incomplete picture of the excitation spectra.

An assignment of the ν_2, ν_4, ν_5, and ν_9 RR excitation spectra of $TCNQ\cdot^-$ produced by $^2B_{3g} \rightarrow {}^2B_{1u}{}^{(1)}$ excitation was carried out. From this assignment it was possible to obtain the frequencies for the two modes most sensitive to electronic structure, ν_2' and ν_4', as well as the frequencies for the structure insensitive modes, ν_3', ν_5', and ν_9', in the $^2B_{1u}{}^{(1)}$ excited state. A qualitative correlation was obtained between CNDO/S calculated π bond order changes and experimental frequency changes for the optical and electron transfer induced electronic structure changes: $TCNQ\cdot^-(^2B_{3g}) + h\nu_0 \rightarrow TCNQ\cdot^-(^2B_{1u}{}^{(1)})$ and $TCNQ\cdot^-(^2B_{3g}) + e^- \rightarrow TCNQ^{2-}(^1A_g)$.

Acknowledgment. The authors wish to thank Professors Abraham Nitzan and Mark Ratner for numerous stimulating discussions. In addition we thank Professor Ratner for access to and assistance in the interpretation of Mr. Karsten Krogh-Jespersen's CNDO/S calculations on $TCNQ\cdot^-$ and $TCNQ^{2-}$ prior to their publication. The support of this research by the National Science Foundation (NSF MPS 7412573) is gratefully acknowledged. One of us (D.L.J.) acknowledges a fellowship from The ACS Analytical Chemistry Division sponsored by The Perkin-Elmer Corp.

References and Notes

(1) Alfred P. Sloan Foundation Fellow, 1974–1976.
(2) H. A. Kramers and W. Heisenberg, *Z. Phys.*, **31**, 681 (1925); P. A. M. Dirac, *Proc. R. Soc. London*, **114**, 710 (1927).
(3) A. C. Albrecht, *J. Chem. Phys.*, **34**, 1476 (1961); J. Tang and A. C. Albrecht, "Raman Spectroscopy", Vol. 2, H. A. Szymanski, Ed., Plenum Press, New York, N.Y., 1970, Chapter 2.
(4) F. A. Savin, *Opt. Spektrosk.*, (*Akad. Nauk SSSR, Otd. Fiz. Mat. Nauk*), **19**, 555 (1965); **19**, 743 (1965); **20**, 549 (1966); *Opt. Spectrosc.* (*USSR*), **19**, 308 (1965); **19**, 412 (1965); **20**, 341 (1966).
(5) E. M. Verlan, *Opt. Spektrosk.* (*Akad. Nauk SSSR, Otd. Fiz. Mat. Nauk*), **20**, 605 (1966); **20**, 802 (1966); *Opt. Spectrosc.* (*USSR*), **20**, 341 (1966); **20**, 447 (1966).
(6) S. Kobinata, *Bull. Chem. Soc. Jpn.*, **46**, 3636 (1973).
(7) J. M. Friedman and R. M. Hochstrasser, *Chem. Phys.*, **1**, 457 (1973).
(8) W. L. Peticolas, L. Nafie, P. Stein, and B. Franconi, *J. Chem. Phys.*, **52**, 1576 (1970).
(9) J. A. Koningstein and B. G. Jakubinek, *J. Raman Spectrosc.*, **2**, 317 (1974); J. A. Koningstein, *Opt. Spectrosc.* (*USSR*), **35**, 260 (1973); J. A. Koningstein, "Introduction to the Theory of the Raman Effect", D. Reidel, Dordrecht, Holland, 1972.
(10) A. C. Albrecht and M. C. Hutley, *J. Chem. Phys.*, **55**, 4438 (1971).
(11) M. Ito and I. Suzuka, *Chem. Phys. Lett.*, **31**, 467 (1975).
(12) M. Mingardi and W. Siebrand, *Chem. Phys. Lett.*, **24**, 492 (1974).
(13) M. Mingardi and W. Siebrand, *J. Chem. Phys.*, **62**, 1074 (1975).
(14) D. Van Labeke, M. Jacon, M. Berjot, and L. Bernard, *J. Raman Spectrosc.*, **2**, 219 (1974).
(15) M. Mingardi, W. Siebrand, D. Van Labeke, and M. Jacon, *Chem. Phys. Lett.*, **31**, 208 (1975).
(16) D. L. Jeanmaire and R. P. Van Duyne, *J. Am. Chem. Soc.*, preceding paper in this issue.
(17) D. L. Jeanmaire, M. R. Suchanski, and R. P. Van Duyne, *J. Am. Chem. Soc.*, **97**, 1699 (1975).
(18) T. C. Strekas, D. H. Adams, A. Packer, and T. G. Spiro, *Appl. Spectrosc.*, **28**, 324 (1974).
(19) D. F. Shriver and J. B. R. Dunn, *Appl. Spectrosc.*, **28**, 319 (1974).
(20) F. C. Strome and S. A. Tuccio, *Opt. Commun.*, **4**, 58 (1971).
(21) W. Kiefer and H. J. Bernstein, *Mol. Phys.*, **23**, 835 (1972).
(22) A. Ranade and M. Stockburger, *Chem. Phys. Lett.*, **22**, 257 (1973).
(23) O. S. Mortensen, *J. Mol. Spectrosc.*, **39**, 48 (1971).
(24) M. Berjot, M. Jacon, and L. Bernard, *Opt. Commun.*, **4**, 117 (1971).
(25) T. G. Spiro, "Chemical and Biochemical Applications of Lasers", C. B. Moore, Ed., Academic Press, New York, N.Y., 1974, Chapter 2.
(26) L. Rimai, R. G. Kilponen, and D. Gill, *J. Am. Chem. Soc.*, **92**, 3824 (1970).
(27) F. Inagaki, M. Tasumi, and T. Miyazawa, *J. Mol. Spectrosc.*, **50**, 286 (1974).
(28) F. Gulluzzi, M. Garozzo, and F. Ricci, *J. Raman Spectrosc.*, **2**, 351 (1974).
(29) B. Gaber, V. Minkowski, and T. G. Spiro, *J. Am. Chem. Soc.*, **96**, 6868 (1974).
(30) RCA data sheet on the C31034 Photomultiplier tube.
(31) J. H. Callomon, T. M. Dunn, and I. M. Mills, *Philos. Trans. R. Soc. London, Ser. A.*, **259**, 499 (1966).
(32) M. R. Suchanski and R. P. Van Duyne, to be published.
(33) M. A. Ratner and K. Krogh-Jespersen, private communication, 1975.
(34) R. E. Long, R. A. Sparks, and K. N. Trueblood, *Acta Crystallogr.*, **18**, 932 (1965).
(35) C. J. Fritchie and P. Arthur, *Acta Crystallogr.*, **21**, 138 (1966).

The Relation of Heat of Vaporization to Surface Tension for Liquids of Nonpolar Spherical Molecules

S. F. Abdulnur

Contribution from the Department of Chemistry, University of New Orleans, Lake Front, New Orleans, Louisiana 70122. *Received August 28, 1975*

Abstract: A relation (eq 6a) between the energy of vaporization and the enthalpy part of surface tension is derived by considering the energy needed to vaporize a molecule from the liquid as equal to that required to create a molecular size spherical cavity within it. It is shown to apply for a variety of nonpolar and polar liquids. Assuming the applicability of macroscopic surface tension values to such dimensions, the radius of the cavity is shown to be that of a hard sphere in a Lennard-Jones 12-6 potential, $\sigma/2$. The relation accounts for Stefan's formula, the empirical relation first obtained by Hildebrand and Scott between surface tension and energy of vaporization, and the negative variation of σ with temperature. A method for obtaining reasonably good estimates of σ from liquid densities is also presented.

I. Introduction

The heat of vaporization of a liquid and its surface tension are macroscopic quantities that reflect the intermolecular forces present in the liquid. The search for a relation between them dates back to the latter part of the 19th century.[1] Such a relation may be derived from first principles through a statistical mechanical treatment of the liquid as a whole.[2] Alternatively, one may achieve this by focusing attention on a single molecule in a cavity in a liquid continuum, as will be shown in the present work. Using such an approach, Stefan in